Differences in phenotype between long-lived memory B cells against *Plasmodium falciparum* merozoite antigens and variant surface antigens

Raphael A. Reyes[1], Louise Turner[2], Isaac Ssewanyana[3], Prasanna Jagannathan[4,5], Margaret E. Feeney[6,7], Thomas Lavstsen[2], Bryan Greenhouse[7], Sebastiaan Bol[1], Evelien M. Bunnik[1]*

[1] Department of Microbiology, Immunology & Molecular Genetics, Long School of Medicine, The University of Texas Health Science Center at San Antonio, San Antonio, TX, USA

[2] Centre for translational Medicine & Parasitology, Department of Immunology and Microbiology, University of Copenhagen, and Department of Infectious Diseases, Righospitalet, Copenhagen, Denmark

[3] Infectious Disease Research Collaboration, Kampala, Uganda

[4] Department of Medicine, Division of Infectious Diseases, Stanford University, Stanford, CA, USA

[5] Department of Microbiology & Immunology, Stanford University, Stanford, CA, USA

[6] Department of Pediatrics, University of California San Francisco, San Francisco, CA, USA

[7] Department of Medicine, University of California San Francisco, San Francisco, CA, USA

*Corresponding author. Email: bunnik@uthscsa.edu

ABSTRACT

Plasmodium falciparum infections elicit strong humoral immune responses to two main groups of antigens expressed by blood-stage parasites: merozoite antigens that are involved in the erythrocyte invasion process and variant surface antigens that mediate endothelial sequestration of infected erythrocytes. Long-lived B cells against both antigen classes can be detected in the circulation for years after exposure, but have not been directly compared. Here, we studied the phenotype of long-lived memory and atypical B cells to merozoite antigens (MSP1 and AMA1) and variant surface antigens (the CIDRα1 domain of PfEMP1) in Ugandan adults before and after local reduction of *P. falciparum* transmission. After a median of 1.7 years without *P. falciparum* infections, the percentage of antigen-specific activated B cells declined, but long-lived antigen-specific B cells were still detectable in all individuals. The majority of MSP1/AMA1-specific B cells were $CD95^{+}CD11c^{+}$ memory B cells, which are primed for rapid differentiation into antibody-secreting cells, and $FcRL5^{-}T\text{-}bet^{-}$ atypical B cells. On the other hand, most CIDRα1-specific B cells were $CD95^{-}CD11c^{-}$ memory B cells. CIDRα1-specific B cells were also enriched among a subset of atypical B cells that seem poised for antigen presentation. These results point to differences in how these antigens are recognized or processed by the immune system and how *P. falciparum*-specific B cells will respond upon re-infection.

INTRODUCTION

Malaria continues to be an enormous public health problem in sub-Saharan Africa (1). This potentially fatal disease is caused by parasites of the *Plasmodium* genus, of which *P. falciparum* is responsible for most malaria cases and deaths (1). The development of an effective vaccine against *P. falciparum* plays an important role in the fight to eradicate malaria. However, a major hurdle to overcome in malaria vaccine development is the quick waning of vaccine-elicited immune responses. Most malaria vaccines and vaccine candidates elicit antibodies that inhibit parasite invasion or development, as well as memory B cells that that will be activated upon the next *P. falciparum* antigen encounter. To improve the durability of malaria vaccine-induced immune responses, it is important to define the characteristics of long-lived anti-parasite immunity (here defined as persisting for at least one year in the absence of exposure), for example by studying long-lived B cell memory induced by *P. falciparum* infection. The goal of this study was to compare long-lived memory B cell responses to different parasite antigens acquired as the result of natural infection in individuals living in a malaria-endemic region.

In the human host, *P. falciparum* develops through several life cycle stages, of which the asexual replication cycle within erythrocytes is responsible for pathogenesis. During this replication cycle, a single *P. falciparum* merozoite infects an erythrocyte and over the course of 48 hours, divides into 16 – 32 daughter cells. These newly formed merozoites then burst out of the infected erythrocyte, each ready to invade a new erythrocyte. People living in malaria-endemic regions are repeatedly infected by *Plasmodium* parasites and, as a result of these repetitive exposures, develop immunoglobulin G (IgG) responses against asexual blood-stage parasites that protect against disease (2,3). The main antigenic targets of these IgG responses can be divided into two categories. The first class are expressed by merozoites and are involved in erythrocyte invasion, such as merozoite surface protein 1 (MSP1) and apical membrane antigen 1 (AMA1). The second class of antigens comprises variant surface antigens that are

expressed by *P. falciparum* on the surface of the infected erythrocyte. The most important of these are members of the *P. falciparum* erythrocyte membrane protein 1 (PfEMP1) family that mediate binding to endothelial receptors on the host microvasculature.

Merozoite-specific memory B cells have been detected in the circulation up to 16 years after infection in the absence of antigen exposure (4–7). Similarly, memory B cells against the PfEMP1 variant VAR2CSA involved in pregnancy-associated malaria can be found in the circulation for many years (8). However, the phenotype of these long-lived *P. falciparum*-specific memory B cells has not been studied in great detail. IgG^+ B cells in the circulation can be divided into two main populations: conventional memory B cells (IgD^-CD27^+) and double negative (DN) B cells (IgD^-CD27^-), both known to harbor *P. falciparum* merozoite antigen-specific B cells (9,10). Recent studies have identified subsets of conventional memory B cells that are associated with durable humoral immune responses after influenza and tetanus vaccination, and SARS-CoV-2 infection (11–14). In particular, the surface protein FcRL5, often expressed in conjunction with the integrin CD11c and the transcription factor T-bet, marks a subset of long-lived class-switched memory B cells that are epigenetically and metabolically poised to differentiate into antibody-secreting cells during recall responses (11). The same three markers are expressed by a subset of DN B cells called DN2 or atypical B cells that are typically expanded in *P. falciparum*-exposed individuals (15,16). Atypical B cells also have the capacity to differentiate into antibody-secreting cells and may thus contribute to protection against malaria (17,18). However, it is unknown whether *P. falciparum*-specific atypical B cells have the same durability as *P. falciparum*-specific memory B cells and if there are differences in the phenotype and longevity of B cells specific for merozoite antigens or variant surface antigens.

In malaria-endemic regions, repetitive *P. falciparum* infections result in boosting of the immune response during every infection. These repeated infections complicate the study of the durability

of anti-parasite immune responses, because every antigen exposure results in the activation and differentiation of long-lived memory B cells and the formation of new memory B cells. To overcome this problem, we used samples that were collected before and after local reduction of *P. falciparum* transmission. Analyzing antigen-specific B cells from these two time points allowed us to evaluate which *P. falciparum*-specific B cell subsets remained present in the absence of new infections and could thus be considered long-lived. Using high parameter spectral flow cytometry, we analyzed the phenotype of memory and atypical B cells that recognize *P. falciparum* merozoite antigens or variant surface antigens. Additionally, we performed an unsupervised clustering analysis of antigen-specific B cells to identify characteristics of the long-lived B cell response that are unique to each class of antigens.

RESULTS

Activated B cell subsets decrease in abundance in the absence of *Plasmodium falciparum* exposure

To study *P. falciparum*-specific B cell responses that were maintained in the absence of new infections, we used peripheral blood mononuclear cells from ten *P. falciparum*-exposed Ugandan adults collected during a period of high *P. falciparum* transmission and after effective mosquito control by means of indoor residual spraying (IRS) had reduced parasite prevalence by 80% (19). Individuals had not tested positive for *P. falciparum* infection for a median of 1.7 years (range, 1.1 – 2.5 years) before collection of blood at the second time point (**Fig. 1**, **Table S1**). B cells were isolated from peripheral blood mononuclear cells and stained with a comprehensive panel of B cell markers (**Table S2**). This panel included antigen tetramers that allowed for the detection of B cells with specificity to two classes of *P. falciparum* antigens: (i) merozoite proteins involved in erythrocyte invasion (merozoite surface protein 1 [MSP1] and apical membrane antigen 1 [AMA1]), and (ii) the cysteine-rich interdomain region α1 (CIDRα1) domain of the variant surface antigen *P. falciparum* erythrocyte membrane protein 1 (PfEMP1)

that is expressed on the surface of the infected erythrocyte. These antigens were selected because we have previously used these proteins to isolate monoclonal antibodies with confirmed antigen specificities (10,20).

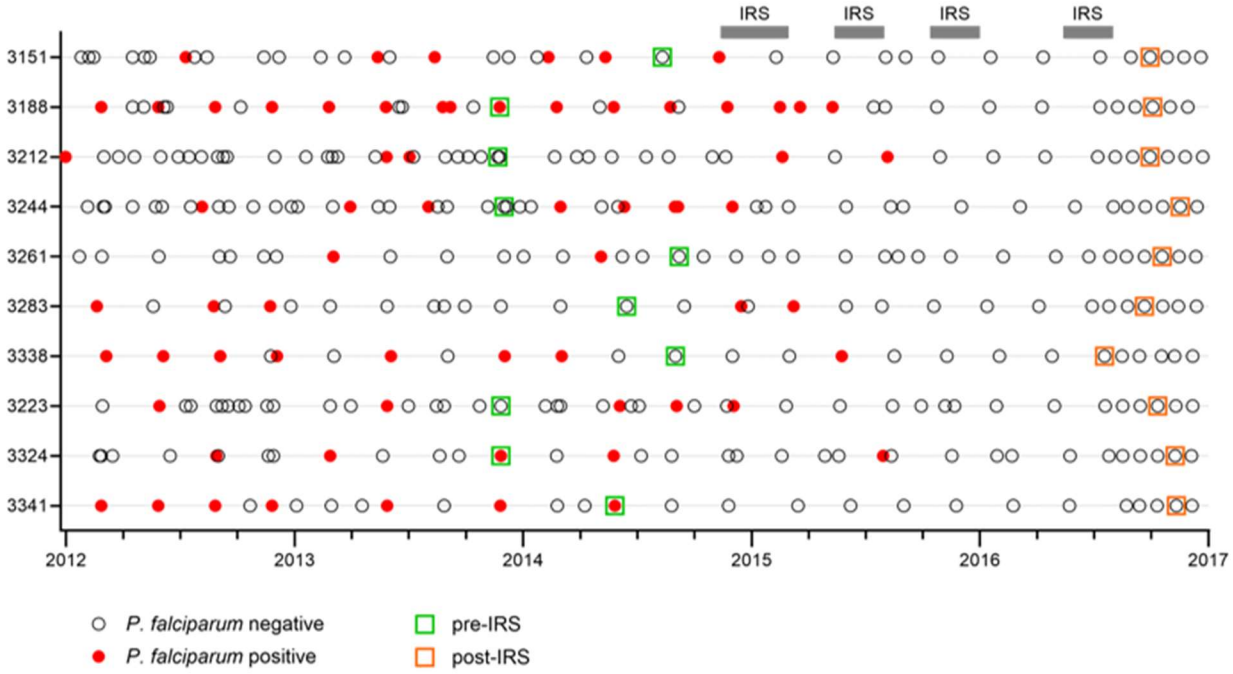

Figure 1: Timing of sample collection. Cohort participants (n = 10) were sampled during routine clinic visits roughly every three months and when they visited a study clinic due to illness. For each visit, the outcome of screening for parasitemia is indicated (open circle for negative, closed red circle for positive). Samples used in this study were collected in late 2013 through late 2014 when *P. falciparum* transmission was high (green squares), and during the second half of 2016 after four rounds of indoor residual spraying (IRS) had reduced *P. falciparum* prevalence by 80% (orange squares). The median time between the last known *P. falciparum* infection and collection of the second sample was 1.7 years.

To assess the composition of the B cell compartment irrespective of antigen-specificity, we first determined the relative abundance of major B cell populations during high *P. falciparum* transmission and after a reduction in parasite exposure. Total $CD19^+$ B cells were divided into naïve B cells (IgD^+CD27^-), unswitched memory B cells (IgD^+CD27^+), switched memory B cells

(IgD$^-$CD27$^+$), and double negative B cells (IgD$^-$CD27$^-$) (**Fig. S1**). Based on the expression of CD11c, naïve B cells were further divided into resting (CD11c$^-$) and activated (CD11c$^+$). For unswitched and switched memory B cell populations, we used CD21 to divide cells into resting (CD21$^+$) and activated (CD21$^-$). Using CD11c and CD21, double negative (DN) B cells were separated into sub-populations DN1, DN2, DN3, and DN4 (**Fig. S1**). DN2 (or atypical; CD11c$^+$CD21$^-$) B cells have been studied extensively in *P. falciparum*-exposed individuals (17,18,21–23), whereas the other three sub-populations of DN B cells have not previously been characterized in the context of malaria. DN1 B cells (CD11c$^-$CD21$^+$) and DN4 (CD11c$^+$CD21$^+$) B cells are thought to be closely related to resting switched memory B cells, while DN3 B cells (CD11c$^-$CD21$^-$) may be precursors of atypical B cells (24,25).

Following IRS, we observed a consistent decrease in the percentage of activated cells: naïve B cells from a median of 5.1% to 2.4% (~55% reduction), unswitched memory B cells from 3.4% to 1.3% (~60% reduction), and switched memory B cells from 12.3% to 7.6% (~40% reduction) (**Fig. 2A, Table S3**). In contrast, the percentage of DN1 cells increased significantly post-IRS, from 2.2% to 3.6% (~40% increase) (**Fig. 2A**). These results are in line with a decrease in immune activation due to an interruption of exposure to *P. falciparum* infections. A similar pattern was observed when we analyzed antigen-specific B cells: the relative abundance of activated, but not resting, MSP1/AMA1-specific and CIDRα1-specific naïve B cells, unswitched memory B cells, and switched memory B cells declined between the two time points (~70, 40, and 75% reduction, respectively for MSP1/AMA1-specific B cells and ~85, 75, and 75% reduction, respectively for CIDRα1-specific B cells) (**Fig. 2B, C**). Additionally, although the total percentage of atypical B cells did not change, the percentage of MSP1/AMA1-specific and CIDRα1-specific atypical B cells decreased (~60% and 65% reduction, respectively). The percentages of antigen-specific DN1, DN3, and DN4 B cells were small and did not change over time (**Fig. 2**, **Fig. S2**). When looking at the abundance of MSP1/AMA1-specific and CIDRα1-

specific B cells among total B cells, we observed that both populations decreased in size, but these differences were not statistically significant (**Fig. 2B, C**).

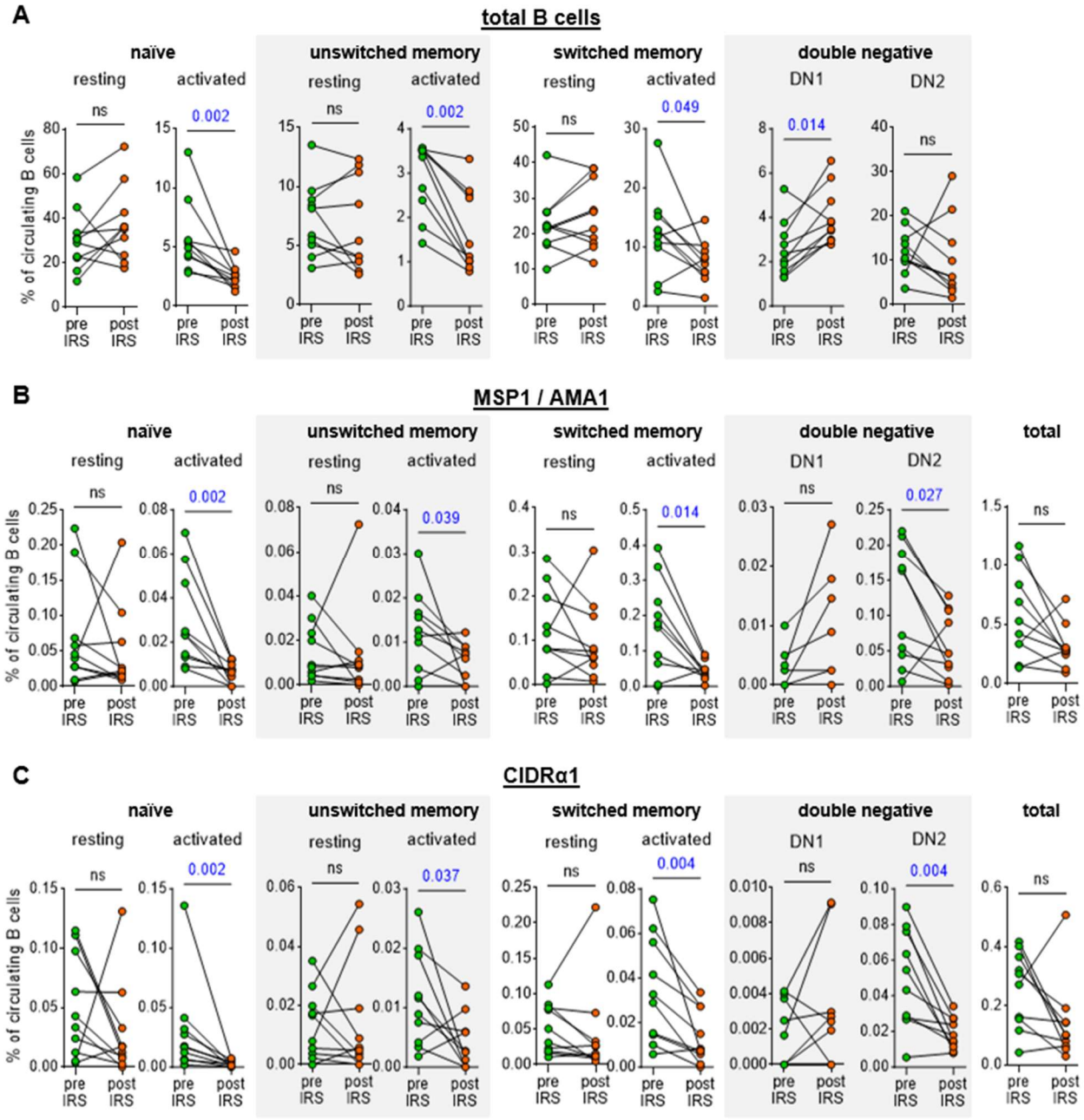

Figure 2: Abundance of total and antigen-specific B cell subsets in the circulation during high parasite transmission and in the absence of *P. falciparum* exposure. The percentage of B cell subsets among circulating B cells is shown for total B cells (A), MSP1/AMA1-specific B cells (B), and CIDRα1-specific B cells (C). For MSP1/AMA1-specific B cells and CIDRα1-specific B cells, the total percentage among all circulating B cells is also shown (right most graphs in each panel). In panels B and C, no antigen-specific DN1 cells were detected pre- and

post-IRS for four individuals. These data points therefore overlap and are not clearly visible. Differences between groups were evaluated using a Wilcoxon matched-pairs signed-rank test. P values < 0.05 are shown in blue. Ns, not significant.

Collectively, these results suggest that the percentage of *P. falciparum*-specific activated B cells declines in the absence of *P. falciparum* infection but that long-lived *P. falciparum*-specific B cells are detectable in the circulation after more than a year without parasite exposure. In addition, we did not observe a difference in the rate at which B cells with specificity for merozoite antigens or variant surface antigens are lost.

Long-lived MSP1/AMA1-specific and CIDRα1-specific B cells differ in phenotype

To further explore similarities and differences in the long-lived memory B cell responses to merozoite antigens and variant surface antigens, we analyzed the phenotype of MSP1/AMA1-specific and CIDRα1-specific B cells. To do this in an unbiased way and without limiting the analysis to pre-defined B cell subsets, we first grouped all non-naïve antigen-specific B cells from all ten individuals at both time points and performed unsupervised clustering based on expression of all markers except Ig isotypes (**Fig. 3A-B, Fig. S3, Table S3**). This analysis identified six clusters, which were classified based on the expression of markers associated with previously characterized B cell populations, as follows: plasmablasts ($CD27^+CD38^+$), activated memory B cells ($CD21^-CD27^+$), two atypical B cell subsets ($CD21^-CD27^-CD11c^+$), and two memory B cell subsets ($CD21^+CD27^+$) (**Fig. 3C**). The two atypical B cell subsets were distinguished by differences in the expression of FcRL5 and T-bet, while the two memory B cell subsets mainly differed in the expression of CD11c, and CD95.

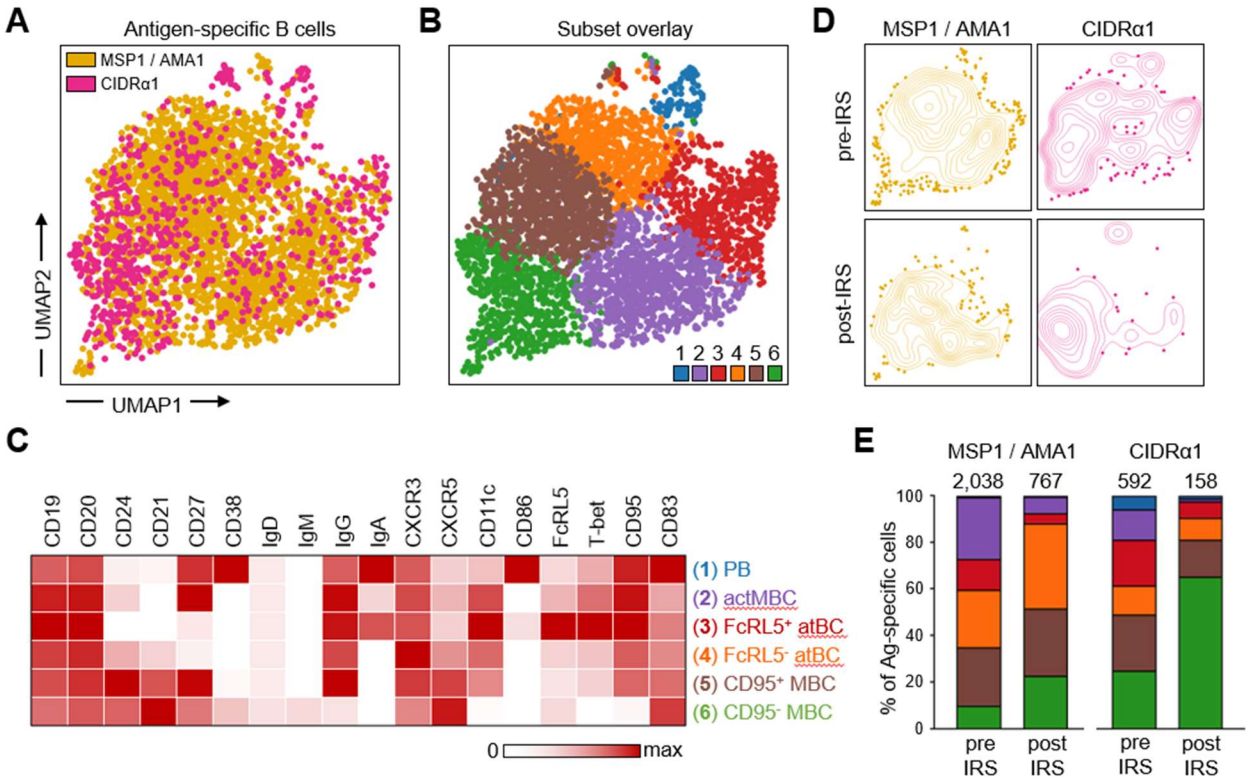

Figure 3: Differences in phenotype between long-lived MSP1/AMA1-specific and CIDRα1-specific B cells. A) Composite UMAP of antigen-specific B cells from samples collected at two time points from 10 individuals, with B cells colored by antigen-specificity. **B)** The same UMAP as shown in panel A with antigen-specific B cells colored by subset. **C)** Median fluorescence intensity of 18 surface and intracellular markers in the six B cell subsets, calculated using flow cytometry data from all 20 samples (two time points for 10 individuals) and color-coded relative to the maximum intensity observed among all B cell populations, including naïve B cells not shown in the heatmap (see Table S3). **D)** Contour plot overlay of MSP1/AMA1-specific and CIDRα1-specific B cells onto the composite UMAP, shown separately for samples collected pre-IRS and post-IRS. **E)** Distribution of all MSP1/AMA1-specific and CIDRα1-specific B cells over the six B cell subsets at the pre-IRS and post-IRS time points. The number above the bar represents the total number of cells. Colors represent the different subsets shown in panel D. PB, plasmablasts; actMBC, activated memory B cells; atBC, atypical B cells; MBC, memory B cells.

Overlay of MSP1/AMA1-specific and CIDRα1-specific B cells onto the composite UMAP of all antigen-specific B cells showed differences in their distribution over the six clusters, especially at the post-IRS time point (**Fig. 3D**). We therefore determined the percentage of antigen-specific cells that belonged to each of the six subsets of B cells (**Fig. 3E**, **Table S3**). This allowed us to

quantify the changes in composition of the MSP1/AMA1-specific and CIDRα1-specific B cells by calculating the percentage overlap between the samples collected before and after IRS. The overlap in composition of CIDRα1-specific B cells between the two time points (60%) was slight lower than that of MSP1/AMA1-specific B cells (71%), suggesting that the population of CIDRα1-specific B cells may have undergone more changes during the period with reduced *P. falciparum* transmission. When comparing the two groups of antigen-specific B cells at each time point, we observed that the populations of MSP1/AMA1-specific and CIDRα1-specific B cells were more similar during high parasite transmission (74%) than in the absence of parasite exposure (54%). Thus, the populations of circulating long-lived B cells with specificity for merozoite antigens or variant surface antigens seem to diverge in their composition in the absence of antigen re-exposure.

To better understand these differences in phenotype between long-lived B cells with different antigen-specificities, we looked more closely at the distribution of MSP1/AMA1-specific and CIDRα1-specific B cells over the six subsets. During a time of high parasite exposure, both MSP1/AMA1-specific and CIDRα1-specific B cells were found among all six subsets. With the exception of plasmablasts that were a small population among both antigen groups, antigen-specific B cells were distributed fairly evenly over the various sub-populations (**Fig. 3E**). In line with the reduction in immune activation, the percentage of short-lived plasmablasts (cluster 1) and activated memory B cells (cluster 2) was lower post-IRS (20 – 70% of the pre-IRS level) (**Fig. 3E**). The same was true for the FcRL5^{+}T-bet^{+} subset of atypical B cells (cluster 3), which decreased in proportion by ~65% for both merozoite and variant surface antigens. However, we observed differences in the relative abundance of subsets 4, 5, and 6 between the two antigen groups. While the fraction of FcRL5^{-}T-bet^{-} atypical B cells (cluster 4) increased among MSP1/AMA1-specific B cells (from 25% pre-IRS to 37% post-IRS), it remained unchanged among CIDRα1-specific B cells (~10%). Additionally, the fraction of CD95^{+}CD11c^{+} memory B

cells (cluster 5) remained stable among MSP1/AMA1-specific B cells (25 – 30%) but decreased among CIDRα1-specific B cells (from 24% pre-IRS to 16% post-IRS). Together, subsets 4 and 5 made up the majority (65%) of MSP1/AMA1-specific B cells post-IRS, but only 25% of CIDRα1-specific B cells at this time point. In contrast, 65% of all CIDRα1-specific B cells detected post-IRS were $CD95^{-}CD11c^{-}$ memory B cells (cluster 6), an almost three-fold increase in comparison to its proportion among CIDRα1-specific B cells present during high *P. falciparum* exposure (25%). Collectively, these results suggest that circulating long-lived anti-*Plasmodium* B cells with different antigen specificities have different phenotypes.

Long-lived MSP1/AMA1-specific memory B cells express CD95 and CD11c

The difference in proportions of $CD95^{+}CD11c^{+}$ (cluster 5) and $CD95^{-}CD11c^{-}$ (cluster 6) long-lived memory B cells between merozoite antigen-specific and variant surface antigen-specific memory B cells was interesting given that, in general, the majority of class-switched memory B cells ($CD19^{+}IgD^{-}CD27^{+}$) do not express these markers (12,14,26). To study this observation in more detail, we determined the percentages of $CD95^{+}$ cells and $CD11c^{+}$ cells among antigen-specific switched memory B cells and the total population of switched memory B cells. Irrespective of the level of parasite exposure, the large majority (80 – 95%) of MSP1/AMA1-specific switched memory B cells expressed CD95, compared to only 40 – 50% of all switched memory B cells (**Fig. 4**). A similar pattern was seen for CD11c with 70 – 80% of MSP1/AMA1-specific switched memory B cells expressing CD11c, compared to only 35 – 40% in the total population of switched memory B cells (**Fig. 4**). During high parasite exposure, the percentages of $CD95^{+}$ / $CD11c^{+}$ MSP1/AMA1-specific switched memory B cells did not differ from those among CIDRα1-specific switched memory B cells (median, 60 – 70%), although it should be mentioned that the percentages of $CD95^{+}$ / $CD11c^{+}$ CIDRα1-specific switched memory B cells were also not statistically different from those of the total population of switched memory B cells (**Fig. 4**). Post-IRS, the percentages of $CD95^{+}$ / $CD11c^{+}$ CIDRα1-specific switched memory B

cells decreased to 25 – 30% and were significantly different from those among MSP1/AMA1-specific switched memory B cells.

CD11c is often co-expressed with FcRL5 and T-bet. Collectively, these markers have been associated with long-lived class-switched memory B cells that participate in robust recall responses (11,12). To determine whether MSP1/AMA1-specific memory B cells not only express higher levels of CD11c than CIDRα1-specific switched memory B cells, but also higher levels of these other two markers, we compared the percentages of FcRL5$^+$ cells and T-bet$^+$ cells among antigen-specific switched memory B cells and the total population of switched memory B cells. The percentage of T-bet$^+$ cells among MSP1/AMA1-specific and CIDRα1-specific switched memory B cells was similar during high parasite exposure (median, 30 – 40%) and post-IRS (median, 5 – 20%), and was not increased as compared to the total population of switched memory B cells (**Fig. 4**). The percentage of cells expressing FcRL5 was low and did not differ between MSP1/AMA1-specific and CIDRα1-specific switched memory B cells (**Fig. 4**). Thus, CD95 and CD11c, but not other markers of durable immunity, are differentially expressed between MSP1/AMA1-specific and CIDRα1-specific long-lived memory B cells.

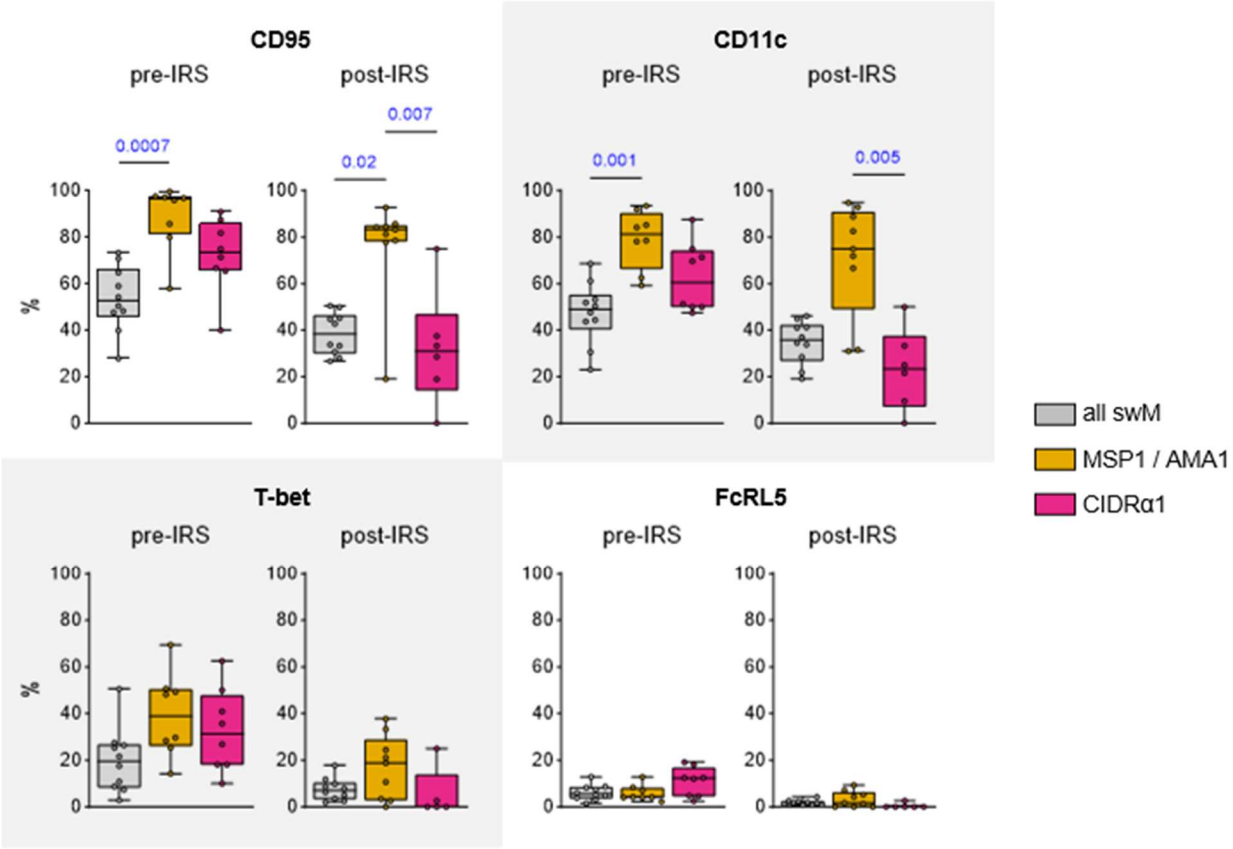

Figure 4: Expression of CD95, CD11c, T-bet, and FcRL5 among long-lived switched memory B cells. The percentage of CD95$^+$, CD11c$^+$, T-bet$^+$, and FcRL5$^+$ cells are shown pre-IRS and post-IRS for all switched memory B cells, as well as MSP1/AMA1-specific and CIDRα1-specific switched memory B cells. Differences between groups were tested using a Kruskal-Wallis test, followed by comparisons between all pairs of groups using Dunn's post-hoc test, which reports P values that have been corrected for multiple comparisons. Only P values < 0.05 are shown. swM, switched memory.

CD86$^+$CD11c^{hi} atypical B cells are enriched for CIDRα1-specific cells

As shown in Figure 3E, we observed that the large majority (90%) of long-lived MSP1/AMA1-specific atypical B cells (clusters 3 and 4, post-IRS) did not express FcRL5 and T-bet, whereas CIDRα1-specific atypical B cells were divided almost equally between the FcRL5$^+$T-bet$^+$ (cluster 3) and FcRL5$^-$T-bet$^-$ (cluster 4) populations. We recently described three subsets of atypical B cells with different functional profiles (18), that we will here refer to as atBC1 (CD86$^+$CD11c^{hi}), atBC2 (CD86$^-$CD11c^{hi}), and atBC3 (CD86$^-$CD11c^{int}). Of these, atBC1 and atBC2 expressed high

levels of FcRL5 and T-bet, whereas atBC3 expressed low levels of T-bet and did not express FcRL5. We determined the proportion of these three previously described subsets of atypical B cells among the MSP1/AMA1-specific atypical B cells and the CIDRα1-specific atypical B cells. After gating on IgD^- atypical B cells ($CD21^-CD27^-CD11c^+IgD^-$), unsupervised clustering was performed, followed by separating the cells into the three atypical B cell subsets based on expression of CD11c and CD86 (**Fig. 5A**, **Fig. S4**). Overall, the fraction of atBC1 among all atypical B cells was smallest (25%) and decreased in the absence of *P. falciparum*-exposure (6%) (**Fig. 5B**). The fraction of atBC2 increased from 27% to 40%, while the relative size of subset atBC3 remained stable at ~50%. However, it is important to note that atypical B cells of all subsets were still detected in the circulation post-IRS, indicating that these cells are long-lived in the absence of infection.

Next, we determined the proportion of MSP1/AMA1-specific and CIDRα1-specific cells among the three atypical B cell subsets, as well as among resting and activated memory B cells. Antigen-specific B cells were found among all atypical and memory B cell populations, but their distributions within each population differed. Resting memory B cells, activated memory B cells, and atBC2 harbored equal proportions of MSP1/AMA1-specific and CIDRα1-specific cells (**Fig. 5C**), suggesting that there is no enrichment for antigen-specificity among these B cell populations. AtBC3 contained about 60% MSP1/AMA1-specific cells and 40% CIDRα1-specific cells, although this difference did not reach statistical significance when analyzed for individual donors (**Fig. S5**). In stark contrast, the majority of antigen-specific atBC1 (~80% after normalizing for the total abundance of MSP1/AMA1-specific and CIDRα1-specific cells) was specific for CIDRα1 at the pre-IRS time point (**Fig. 5C, Fig. S5**). The relative abundance of CIDRα1-specific cells within atBC1 was even higher post-IRS, although it should be noted that very few antigen-specific B cells were detected at this time point (10 cells in total). Collectively, these results suggest that atypical B cells are part of the long-lived B cell response to

328 *Plasmodium* antigens and point to differences in the atypical B cell response to different classes
329 of antigens.
330

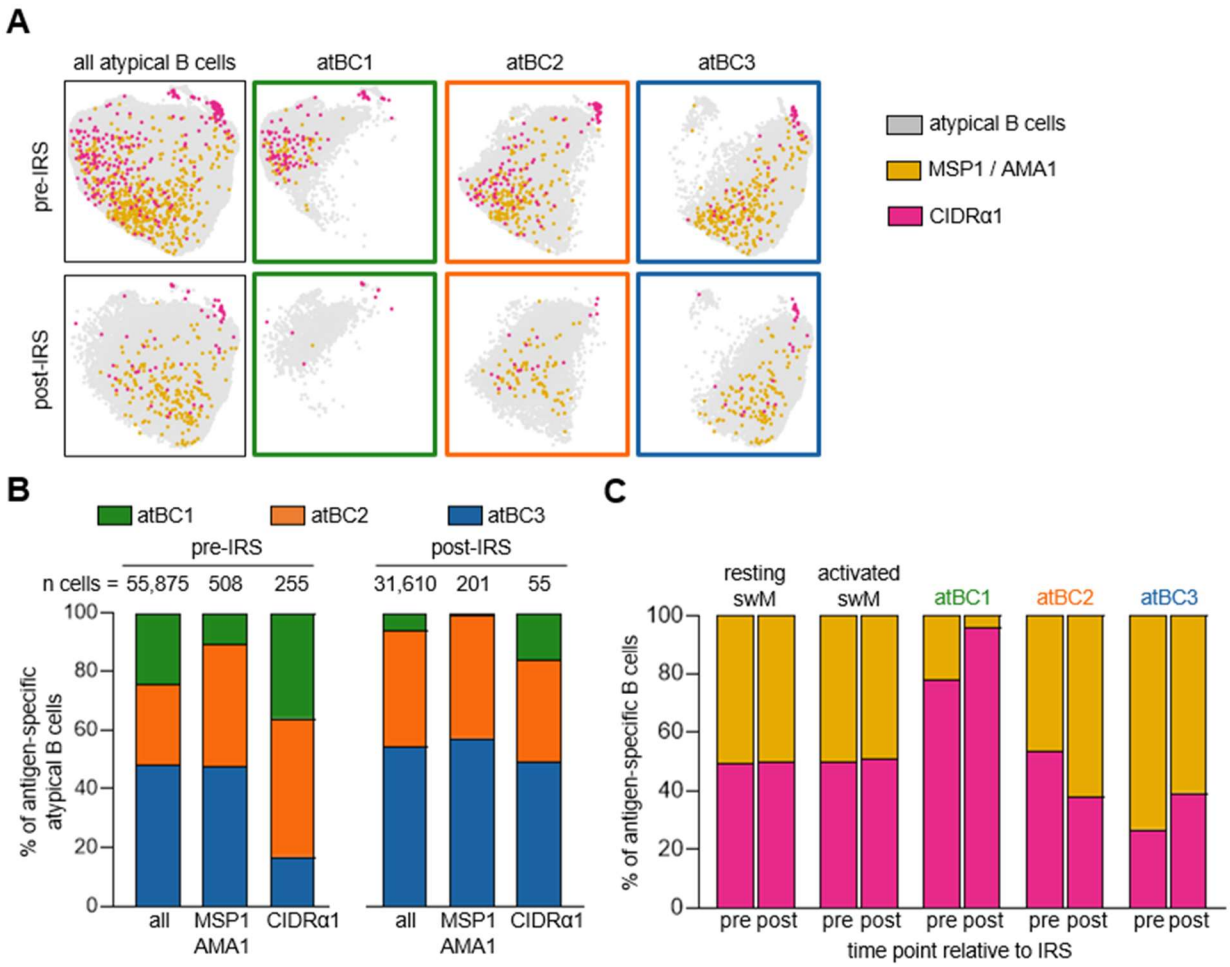

331

332 **Figure 5: Distribution of MSP1/AMA1-specific and CIDRα1-specific B cells among**
333 **atypical B cell subsets. A)** Composite UMAP of atypical B cells from samples collected at two
334 time points from 10 individuals, separated by time point (left column). UMAPs for each of the
335 three atypical B cell subsets are also shown (right three columns in green, orange, and blue).
336 MSP1/AMA1-specific and CIDRα1-specific B cells were projected onto these UMAPs. **B)**
337 Distribution of MSP1/AMA1-specific and CIDRα1-specific B cells over the three atypical B cell
338 subsets in samples collected during times of frequent *P. falciparum* infection (pre-IRS) and in
339 absence of parasite infection (post-IRS). **C)** The normalized percentage of MSP1/AMA1-specific
340 and CIDRα1-specific B cells among different B cell subsets. swM, switched memory B cell;
341 atBC*i*, atypical B cell subset *i*.
342

343

DISCUSSION

Our current understanding of the longevity of naturally acquired immunity against *P. falciparum* is mostly based on studies that measured the presence of anti-parasite antibodies in serum. Previous research on memory B cell responses in *P. falciparum*-exposed individuals has mainly focused on changes in the major B cell populations shortly after acute infection or on studying B cell memory in non-immune individuals (4,27,28). In recent years, novel subsets of memory and atypical B cells have been discovered, each of which may play a different role in the immune response to infection (11–14,18). To identify components of the naturally acquired B cell response that contribute to long-lived memory against *P. falciparum* infection, we studied samples collected from individuals living in a malaria endemic region before and after a reduction in *P. falciparum* exposure due to highly effective vector control. Using spectral flow cytometry, we determined the phenotype of B cells with specificity to *P. falciparum* merozoite antigens (MSP1/AMA1) and variant surface antigens (the CIDRα1 domain of PfEMP1). While both groups of antigen-specific B cells showed similar dynamics over time (i.e., a reduction in the percentage of activated B cells), we observed several differences in the composition of circulating long-lived MSP1/AMA1-specific B cells and CIDRα1-specific B cells.

First, we found that the majority of MSP1/AMA1-specific switched memory B cells expressed CD95 and CD11c. CD95 is a death receptor that can induce apoptosis of the cell when it gets bound by its ligand. CD95 is upregulated in germinal center B cells and activated B cells as a mechanism to regulate the humoral immune response and limit inflammation (29). Seemingly contradictory, it can also play a role in cell survival and proliferation (30). Until now, it was unclear whether $CD95^{+}$ cells were recent germinal center emigrants that would disappear shortly after the resolution of infection, or whether they were part of a durable memory B cell response. Our observation that approximately 80% of MSP1/AMA1-specific switched memory B cells expressed CD95 after almost two years without *P. falciparum* exposure suggests that

these cells are long-lived in the circulation. Glass *et al.* showed that CD95$^+$ memory B cells were phenotypically more closely related to plasma cells than other memory B cell subsets, suggesting that these cells readily differentiate into antibody-secreting cells upon antigen encounter (26). Indeed, CD95$^+$ memory B cells strongly responded to BCR crosslinking, resulting in the phosphorylation of proteins that are part of the BCR signaling cascade (26). CD11c expression has also been shown to be upregulated by BCR stimulation, and, similar to CD95$^+$ memory B cells, CD11c$^+$ B cells are more prone to differentiate into antibody-secreting cells than CD11c$^-$ B cells (31). Together, this suggests that MSP1/AMA1-specific switched memory B cells are enriched for an effector memory population that will rapidly differentiate into antibody-secreting cells upon antigen encounter. Interestingly, long-lived MSP1/AMA1-specific switched memory B cells did not express FcRL5 or T-bet, markers that are often co-expressed with CD11c and have been associated with durable B cell immunity and rapid recall responses following vaccination (11,12). The lack of FcRL5 and T-bet expression in CD11c$^+$ memory B cells observed here may point to differences in the immune response to vaccination and infection.

The second major difference between MSP1/AMA1-specific B cells and CIDRα1-specific B cells was that the large majority of atypical B cells subset 1 were CIDRα1-specific. We previously reported that this subset of atypical B cells had the most “atypical” phenotype, with highest expression of CD19, CD11c, FcRL5, and T-bet, and upregulated many genes that are involved in antigen presentation and interaction with T cells (18). This subset of atypical B cells is most likely to home to the spleen where they function as a memory B cell subset, possibly to rapidly respond to systemic infections (32,33). Their presence in the circulation may be the result of spillover from the spleen, either due to limited space to harbor all newly formed atypical B cells or to distortion of the spleen architecture during *P. falciparum* infections (34). In the circulation, the proportion of this atypical B cell subset decreased after a period without *P. falciparum*

infection. However, it is possible that these cells are longer-lived in the spleen and are more abundant than can be assessed using PBMCs.

What may underlie the differences in phenotype between MSP1/AMA1-specific and CIDRα1-specific memory B cells? One possible explanation may be a difference in the type of cell that initially captures the antigen for presentation to $CD4^+$ T cells. MSP1 and AMA1 are both shed from the merozoite surface during invasion and are thus present in the circulation in soluble form (35). Dendritic cells are highly efficient at taking up and presenting soluble antigen (36). In contrast, PfEMP1 is expressed on the surface of infected erythrocytes, which can be considered 'particles'. Dendritic cells have been shown to be dispensable for mounting an immune response to particulate antigens (37). Instead, B cells are the primary antigen-presenting cells that take up particulate antigens, including *Plasmodium*-infected erythrocytes (36–38). Gao *et al.* recently showed that atypical B cells were better at presenting antigen and activating $CD4^+$ T cells than other B cell subsets (39). In line with these observations, we show that atypical B cell subset 1 (that seems primed for antigen presentation) was enriched for particle-associated CIDRα1-specific B cells over B cells with specificity for soluble antigens MSP1 and AMA1, suggesting that capturing infected erythrocytes and presenting parasite antigens to T cells may be an important function of this atypical B cell subset. We have previously determined that this subset of atypical B cells can also be stimulated to differentiate into antibody-secreting cells in vitro (18), indicating that it may have dual roles in the immune response to *P. falciparum*.

Another explanation for the observed differences in phenotype of antigen-specific B cells is that certain B cell receptor properties predispose B cells to a certain fate. It has been hypothesized that atypical B cells are derived from anergic cells with low levels of autoreactivity (40). During *P. falciparum* infection, these cells could be activated and acquire mutations in the B cell receptor that increase their affinity to *P. falciparum* antigens and at the same time decrease

their autoreactivity (40). In line with this theory, we have previously observed differences in antibody heavy chain V-gene usage between memory and atypical B cells (41). Specifically, we showed that V_H3-48 was overrepresented among IgG^+ atypical B cells. Interestingly, we have recently isolated two broadly inhibitory antibodies against CIDRα1 that both used V_H3-48 (20). These observations suggest that intrinsic autoreactivity of their B cell receptor may equip atypical B cells with the potential to recognize *P. falciparum* variant surface antigens.

Finally, it cannot be ruled out that *P. falciparum*-exposed individuals have different life-time levels and frequencies of exposure to these two groups of antigens that may result in differences in phenotypes of long-lived B cells. With every asexual replication cycle of blood-stage *P. falciparum*, MSP1 and AMA1 are expressed to mediate erythrocyte invasion. B cell responses against these two antigens are thus expected to get boosted with every *P. falciparum* infection. On the other hand, not all PfEMP1 variants contain a CIDRα1 domain (42). Although the parasite population within an infected individual may collectively express multiple PfEMP1 variants, it is possible that not every infection leads to exposure of the immune system to CIDRα1. However, we observed a similar reduction of activated MSP1/AMA1-specific and CIDRα1-specific cells from the pre-IRS to the post-IRS time point among all major B cell populations: naïve, unswitched memory, switched memory, and atypical B cells. In addition, the unsupervised clustering analysis of antigen-specific B cells identified a population of CIDRα1-specific plasmablasts that were short-lived in the circulation. Together, these observations suggest that the individuals in this study had recently been exposed to CIDRα1 and that a lack of CIDRα1 exposure in itself cannot explain the differences in long-lived memory B cell responses between CIDRα1 and merozoite antigens.

This study has several limitations. First, the study population is relatively small and homogeneous (ten women between 25 and 65 years of age). Performing a similar analysis in a

larger cohort of individuals of different age groups, including children and men, will strengthen our observations. Second, we assessed B cell responses almost 1.5 – 2 years after the last known *P. falciparum* infection, which is a relatively short time without antigen exposure. Long-lived memory B cells have been detected decades after infection or vaccination (4–8,43). It would be interesting to survey the ten individuals included in this study again at a later time point. Third, our analyses are restricted to B cell phenotype and did not include functional assessment of the various B cell populations identified here. Finally, we detected relatively few antigen-specific B cells, especially for CIDRα1 in the absence of *P. falciparum* exposure, which prevented us from analyzing responses for each person separately. Instead, we aggregated antigen-specific B cells from ten individuals and analyzed them in bulk. Using antigen probes of additional CIDRα1 variants and non-3D7 *P. falciparum* MSP1/AMA1 variants could facilitate the detection of larger numbers of antigen-specific B cells.

In conclusion, we analyzed long-lived B cell responses against merozoite antigens and variant surface antigens in individuals living in a malaria-endemic region at a time when *P. falciparum* transmission was high, and after at least a year (median of 1.7 years) without parasite exposure. The loss of MSP1/AMA1-specific and CIDRα1-specific B cells in the circulation was similar, but the phenotype of long-lived MSP1/AMA1-specific and CIDRα1-specific B cells was different. The majority of long-lived MSP1/AMA1-specific were $CD95^{+}CD11c^{+}$ memory B cells and $FcRL5^{-}T\text{-}bet^{-}$ atypical B cells, whereas the majority of long-lived CIDRα1-specific B cells were $CD95^{-}CD11c^{-}$ memory B cells. Our results do not necessarily point to a qualitative difference in the memory B cell response to these antigens but may be reflective of differences in how these different antigens are recognized or processed by the immune system, and how the immune response will unfold during a new *P. falciparum* infection.

MATERIALS AND METHODS

Study design and ethics approval

All ten individuals included in this study were residents of the Nagongera sub-county in Tororo District, Uganda. This region was historically characterized by extremely high *P. falciparum* transmission intensity, with an estimated annual entomological inoculation rate of 125 infectious bites per person per year (44). Since 2015, multiple rounds of indoor residual spraying (IRS) have dramatically reduced malaria incidence compared with pre-IRS levels (19). Individuals were selected for inclusion into this study based on age and *P. falciparum* exposure. All individuals included in this study were enrolled in The Program for Resistance, Immunology, Surveillance, and Modeling of Malaria (PRISM) program (45) and have provided written consent for the use of their samples for research. The PRISM cohort study was approved by the Makerere University School of Medicine Research and Ethics Committee (SOMREC), London School of Hygiene and Tropical Medicine IRB, the University of California, San Francisco Human Research Protection Program, and the Stanford University School of Medicine IRB. The use of cohort samples for this study was approved by the Institutional Review Board of the University of Texas Health Science Center at San Antonio.

B cell isolation

Cryopreserved PBMCs were thawed and immediately mixed with pre-warmed (37˚C) thawing medium (IMDM/GlutaMAX supplemented with 10% heat-inactivated FBS (USA origin) and 0.01% Universal Nuclease (Thermo, #88700)) to wash away the DMSO. After centrifugation (250 × g, 5 min at RT), the cell pellet was resuspended in warm thawing medium and viable cells were counted. Next, cells were centrifuged (250 × g, 5 min at RT), resuspended in isolation buffer (PBS with 2% FBS and 1 mM (f/c) EDTA) at 50 million live cells/mL, and filtered through a 35 µm sterile filter cap (Corning, # 352235) to break apart any aggregated PBMCs. B cells were isolated by negative selection using the EasySep Human B Cell Isolation Kit (StemCell, #17954)

or the MojoSort Human Pan B Cell Isolation Kit (BioLegend, # 480082) according to the manufacturer's instructions.

Staining for spectral flow analysis

C-terminally biotinylated full-length *P. falciparum* 3D7 MSP1 and AMA1 were produced in Expi293F cells (Thermo, # A14635) as described previously (10). C-terminally StrepTagII labeled HB3VAR03 CIDRα1.4 and IT4VAR20 CIDRα1.1 were produced in baculovirus-infected insect cells as described previously (46). Antigen tetramers were synthesized by incubating protein with fluorophore-conjugated streptavidin overnight at 4˚C at a molar ratio of 6:1 with rotation. MSP1 and AMA1 tetramers were made with APC-conjugated streptavidin (Cytek, # 20-4317-U100) and BUV563-conjugated streptavidin (BD, # 612935), while CIDRα1 tetramers were generated with PE-labeled streptavidin (Cytek, # 50-4317-U100) and BUV661-conjugated streptavidin (BD, # 612979). B cells isolated by negative selection were washed with PBS, centrifuged (250 × g, 5 min), resuspended in 1 ml of PBS containing 1 µl live/dead stain (Zombie UV Fixable Viability kit (Biolegend, # 423107)) and incubated on ice for 30 min. Cells were subsequently washed with cold PBS containing 1% BSA (250 × g, 5 min, 4ºC), resuspended with a cocktail of 25 µM of each merozoite tetramer (MSP1/AMA1) diluted in PBS containing 1% BSA to a volume of 100 µl, and incubated at 4°C for 30 min. The cells were then washed twice with cold PBS containing 1% BSA (250 × g, 5 min, 4ºC) and incubated with a cocktail of 25 µM of each CIDRα1 tetramer (CIDRα1.1/ CIDRα1.4) diluted in PBS containing 1% BSA to a volume of 100 µl, and incubated at 4°C for 30 min. Next, the cells were washed twice with cold PBS containing 1% BSA (250 × g, 5 min, 4ºC) and incubated at 4°C for 30 min with a B cell surface marker antibody cocktail (**Table S2**) with 10 µl Brilliant Stain Buffer Plus (BD, # 566385) diluted in PBS containing 1% BSA up to a volume of 100 µl. The cells were then washed with cold PBS containing 1% BSA (250 × g, 5 min, 4ºC), resuspended in 1 ml of Transcription Factor Fix/Perm Concentrate (Cytek, part of # TNB-0607-KIT), diluted with 3 parts

Transcription Factor Fix/Perm Diluent (Cytek), and incubated at 4°C for 1 hour. After the incubation, the cells were washed twice with 3 ml of 1× Flow Cytometry Perm Buffer (Cytek) (300 × g, 8 min, 4ºC) and resuspended in 1× Flow Cytometry Perm Buffer with an anti-human T-bet antibody. After an incubation at 4°C for 30 min, the cells were washed twice with 3 ml cold 1× Flow Cytometry Perm Buffer (300 × g, 8 min, 4ºC) and once with 3 ml cold PBS containing 1% BSA, resuspended in cold PBS containing 1% BSA to 20 – 30 million cells/ml and filtered into a FACS tube through a 35 µm sterile filter cap. Cells were analyzed by flow cytometry immediately following intracellular staining.

Spectral flow cytometry analysis

B cells were analyzed on a Cytek Aurora spectral flow cytometer equipped with five lasers. SpectroFlo QC Beads (Cytek, # N7-97355) were run prior to each experiment for routine performance tracking. Daily quality control and Levey-Jennings tracking reports were used to ensure optimal performance of the machine and to confirm that settings between different runs were comparable. Pooled B cells from two malaria-naïve US donors were used for the unstained control, technical replicates, and to perform compensation for the live/dead stain. UltraComp eBeads Plus Compensation Beads (Thermo, #01-3333-41) were used to perform compensation for all other fluorophores. Between experiments performed on different days, the technical replicates showed near perfect correlation between the expression of cell surface and intracellular markers (Spearman r = 0.98). To minimize experimental variation, paired samples were analyzed within the same experiment.

The cytometry analysis software OMIQ (Dotmatics) was used for all data analysis. B cell subsets and antigen specific B cells were manually gated in OMIQ (**Figure S1**). Since both MSP1 and AMA1 tetramers were generated in the same two fluorochrome format (APC and BUV563), MSP1/AMA-specific B cells were collectively defined as cells staining positive for both

552 tetramer formats. For CIDRα1, we used the domain variants IT4VAR20 CIDRα1.1, HB3VAR03
553 CIDRα1.4, and IT4VAR22 CIDRα1.7 that are highly diverse in sequence. Because tetramers for
554 each CIDRα1 variant were generated using PE and BUV661 fluorochromes, B cells binding
555 either one of the two variants were indistinguishable. Therefore, all CIDRα1.1, CIDRα1.4, and
556 CIDRα1.7-reactive B cells were collectively referred to as CIDRα1-specific B cells. Antigen-
557 specific B cells were defined as cells staining positive for both tetramer formats in a single
558 antigen group. To exclude any non-specific binders, B cells with reactivity to both MSP1/AMA1
559 and CIDRα1 probes were removed. Thus, the gating strategy for antigen-specific B cells is
560 summarized as follows: single / live / $CD19^+$ / $CD20^+$ / IgD- / non-strep / (MSP1/AMA1+ or
561 CIDRα1+).
562
563 Data integration and dimension reduction analysis were performed using Uniform Manifold
564 Approximation and Projection (UMAP). UMAPs of antigen-specific B cells were created using
565 the expression of CD19, CD20, CD21, CD24, CD27, CD38, CD83, CD86, CD95, CXCR3,
566 CXCR5, CD11c, FcRL5, and T-bet as features with default parameters (neighbors = 15,
567 minimum distance = 0.8, metric = Euclidean, random seed = 2478) and included all 20 Ugandan
568 donor samples used in this study for initial projection. FlowSOM (47) was used to identify six cell
569 subsets based on the expression of CD19, CD20, CD21, CD24, CD27, CD38, CD83, CD86,
570 CD95, CXCR3, CXCR5, CD11c, FcRL5, and T-bet (metric = Elucidean, random seed = 1150).
571 For the analysis of atypical B cells, atypical B cells were pre-gated on single / live / $CD19^+$ /
572 $CD20^+$ / $CD21^-$ / $CD27^-$ / $CD11c^+$ / IgD^- cells, followed by the generation of a UMAP (neighbors =
573 15, minimum distance = 0.8, metric = Euclidean, random seed = 2742) based on the expression
574 of markers associated with atypical B cells (CD19, CD20, CD24, CD38, CD86, CD95, CXCR3,
575 CXCR5, CD11c, FcRL5, and T-bet). To define the three atypical B cell subsets, FlowSOM (47)
576 was used to identify three clusters based on CD11c and CD86 expression using default
577 parameters (metric = Euclidean, random seed = 7333). For the projection of antigen-specific B

578 cells onto the UMAP, gates were manually set to identify populations of interest using two-
579 dimensional displays, which were then overlaid onto the UMAP projection. Mean fluorescence
580 intensities of cell surface and intracellular markers in select B cell subsets were calculated using
581 the heatmap function in OMIQ. For the analysis of expression of individual markers (CD95,
582 CD11c, T-bet, and FcRL5) in switched memory B cells, samples with fewer than 10 cells were
583 excluded from analysis.
584
585 **Percent overlap in B cell populations**
586 To determine the similarity in distribution of MSP1/AMA1-specific and CIDRα1-specific B cells
587 over six B cell subsets, we calculated the percentage overlap between pair-wise combinations
588 of samples. For each subset, we determined which of the two samples had the smallest fraction
589 of that subset. For example, if subset A took up 25% of sample x and 17% of sample y, we used
590 the value of 17%. We then calculated the sum of these six smallest fractions to obtain the
591 overlap in composition between the two samples. All distributions and calculations of percent
592 overlap are included in **Table S3**.
593
594 **Statistical analysis**
595 Statistical analyses of flow cytometry data were performed in GraphPad Prism 10 with details of
596 statistical tests provided in the relevant figure legends. P values < 0.05 were considered
597 statistically significant.
598

599 **Acknowledgements**

600 This work was supported by the National Institutes of Health (R01 AI153425 to EMB, F31
601 AI169993 to RAR, TL1 TR002647 to RAR, U19 AI150741 to BG and PJ, and U19 AI089674).
602 Data were generated in the Flow Cytometry Shared Resource at UT Health San Antonio, which

603 is supported by a grant from the National Cancer Institute (P30CA054174) to the Mays Cancer
604 Center, a grant from the Cancer Prevention and Research Institute of Texas (CPRIT)
605 (RP210126), a grant from the National Institutes of Health (S10OD030432), and support from
606 the Office of the Vice President for Research at UT Health San Antonio. Plasmids encoding 3D7
607 MSP1-bio, AMA1-bio, and BirA, were a kind gift from Dr. Gavin Wright (Wellcome Sanger
608 Institute).

609

610 **Author contributions**

611 R.A.R. performed spectral flow cytometry experiments and data analysis. L.T. and T.L. provided
612 CIDRα1 proteins. I.S., P.J., M.E.F., and B.G. provided clinical samples. R.A.R., S.B., and
613 E.M.B. wrote the manuscript with input from all other co-authors. All authors contributed to the
614 article and approved the submitted version.

615

616 **References**

617 1. World malaria report 2023 [Internet]. [cited 2024 Mar 12]. Available from:
618 https://www.who.int/teams/global-malaria-programme/reports/world-malaria-report-2023
619 2. Dent AE, Nakajima R, Liang L, Baum E, Moormann AM, Sumba PO, et al. Plasmodium
620 falciparum Protein Microarray Antibody Profiles Correlate With Protection From
621 Symptomatic Malaria in Kenya. J Infect Dis. 2015 Nov 1;212(9):1429–38.
622 3. Crompton PD, Kayala MA, Traore B, Kayentao K, Ongoiba A, Weiss GE, et al. A
623 prospective analysis of the Ab response to Plasmodium falciparum before and after a
624 malaria season by protein microarray. Proc Natl Acad Sci. 2010 Apr 13;107(15):6958–63.
625 4. Ndungu FM, Lundblom K, Rono J, Illingworth J, Eriksson S, Färnert A. Long-lived
626 Plasmodium falciparum specific memory B cells in naturally exposed Swedish travelers. Eur
627 J Immunol. 2013;43(11):2919–29.
628 5. Ndungu FM, Olotu A, Mwacharo J, Nyonda M, Apfeld J, Mramba LK, et al. Memory B cells
629 are a more reliable archive for historical antimalarial responses than plasma antibodies in
630 no-longer exposed children. Proc Natl Acad Sci. 2012 May 22;109(21):8247–52.
631 6. Ayieko C, Maue AC, Jura WGZO, Noland GS, Ayodo G, Rochford R, et al. Changes in B
632 Cell Populations and Merozoite Surface Protein-1-Specific Memory B Cell Responses after
633 Prolonged Absence of Detectable P. falciparum Infection. PLOS ONE. 2013 Jun
634 27;8(6):e67230.

7. Wipasa J, Suphavilai C, Okell LC, Cook J, Corran PH, Thaikla K, et al. Long-Lived Antibody and B Cell Memory Responses to the Human Malaria Parasites, Plasmodium falciparum and Plasmodium vivax. PLOS Pathog. 2010 Feb 19;6(2):e1000770.
8. Ampomah P, Stevenson L, Ofori MF, Barfod L, Hviid L. B-Cell Responses to Pregnancy-Restricted and -Unrestricted Plasmodium falciparum Erythrocyte Membrane Protein 1 Antigens in Ghanaian Women Naturally Exposed to Malaria Parasites. Infect Immun. 2014 Apr 18;82(5):1860–71.
9. Hopp CS, Sekar P, Diouf A, Miura K, Boswell K, Skinner J, et al. Plasmodium falciparum–specific IgM B cells dominate in children, expand with malaria, and produce functional IgM. J Exp Med. 2021 Mar 4;218(4):e20200901.
10. Gonzales SJ, Clarke KN, Batugedara G, Garza R, Reyes RA, Ssewanyana I, et al. A Molecular Analysis of Memory B Cell and Antibody Responses Against Plasmodium falciparum Merozoite Surface Protein 1 in Children and Adults From Uganda. Front Immunol [Internet]. 2022 Jun 2 [cited 2024 Mar 12];13. Available from: https://www.frontiersin.org/journals/immunology/articles/10.3389/fimmu.2022.809264/full
11. Nellore A, Zumaquero E, Scharer CD, Fucile CF, Tipton CM, King RG, et al. A transcriptionally distinct subset of influenza-specific effector memory B cells predicts long-lived antibody responses to vaccination in humans. Immunity. 2023 Apr 11;56(4):847-863.e8.
12. Kim CC, Baccarella AM, Bayat A, Pepper M, Fontana MF. FCRL5+ Memory B Cells Exhibit Robust Recall Responses. Cell Rep. 2019 Apr 30;27(5):1446-1460.e4.
13. Ogega CO, Skinner NE, Blair PW, Park HS, Littlefield K, Ganesan A, et al. Durable SARS-CoV-2 B cell immunity after mild or severe disease. J Clin Invest [Internet]. 2021 Apr 1 [cited 2024 Mar 12];131(7). Available from: https://www.jci.org/articles/view/145516
14. Reyes RA, Clarke K, Gonzales SJ, Cantwell AM, Garza R, Catano G, et al. SARS-CoV-2 spike-specific memory B cells express higher levels of T-bet and FcRL5 after non-severe COVID-19 as compared to severe disease. PLOS ONE. 2021 Dec 22;16(12):e0261656.
15. Weiss GE, Traore B, Kayentao K, Ongoiba A, Doumbo S, Doumtabe D, et al. The Plasmodium falciparum-Specific Human Memory B Cell Compartment Expands Gradually with Repeated Malaria Infections. PLOS Pathog. 2010 May 20;6(5):e1000912.
16. Weiss GE, Crompton PD, Li S, Walsh LA, Moir S, Traore B, et al. Atypical Memory B Cells Are Greatly Expanded in Individuals Living in a Malaria-Endemic Area1. J Immunol. 2009 Aug 1;183(3):2176–82.
17. Hopp CS, Skinner J, Anzick SL, Tipton CM, Peterson ME, Li S, et al. Atypical B cells up-regulate costimulatory molecules during malaria and secrete antibodies with T follicular helper cell support. Sci Immunol. 2022 May 13;7(71):eabn1250.
18. Reyes RA, Batugedara G, Dutta P, Reers AB, Garza R, Ssewanyana I, et al. Atypical B cells consist of subsets with distinct functional profiles. iScience. 2023 Dec 15;26(12):108496.
19. Kamya MR, Kakuru A, Muhindo M, Arinaitwe E, Nankabirwa JI, Rek J, et al. The Impact of Control Interventions on Malaria Burden in Young Children in a Historically High-Transmission District of Uganda: A Pooled Analysis of Cohort Studies from 2007 to 2018. Am J Trop Med Hyg. 2020 May 18;103(2):785–92.
20. Reyes RA, Raghavan SSR, Hurlburt NK, Introini V, Kana IH, Jensen RW, et al. Broadly inhibitory antibodies against severe malaria virulence proteins [Internet]. bioRxiv; 2024 [cited 2024 Apr 5]. p. 2024.01.25.577124. Available from: https://www.biorxiv.org/content/10.1101/2024.01.25.577124v1
21. Portugal S, Tipton CM, Sohn H, Kone Y, Wang J, Li S, et al. Malaria-associated atypical memory B cells exhibit markedly reduced B cell receptor signaling and effector function. Krzych U, editor. eLife. 2015 May 8;4:e07218.

22. Holla P, Dizon B, Ambegaonkar AA, Rogel N, Goldschmidt E, Boddapati AK, et al. Shared transcriptional profiles of atypical B cells suggest common drivers of expansion and function in malaria, HIV, and autoimmunity. Sci Adv. 2021 May 26;7(22):eabg8384.
23. Sullivan RT, Kim CC, Fontana MF, Feeney ME, Jagannathan P, Boyle MJ, et al. FCRL5 Delineates Functionally Impaired Memory B Cells Associated with Plasmodium falciparum Exposure. PLOS Pathog. 2015 May 19;11(5):e1004894.
24. Woodruff MC, Ramonell RP, Haddad NS, Anam FA, Rudolph ME, Walker TA, et al. Dysregulated naive B cells and de novo autoreactivity in severe COVID-19. Nature. 2022 Nov;611(7934):139–47.
25. Stewart A, Ng JCF, Wallis G, Fraternali F, Dunn-Walters DK. Single-Cell Transcriptomic Analyses Define Distinct Peripheral B Cell Subsets and Discrete Development Pathways. Front Immunol [Internet]. 2021 Mar 18 [cited 2024 Mar 13];12. Available from: https://www.frontiersin.org/journals/immunology/articles/10.3389/fimmu.2021.602539/full
26. Glass DR, Tsai AG, Oliveria JP, Hartmann FJ, Kimmey SC, Calderon AA, et al. An Integrated Multi-omic Single-Cell Atlas of Human B Cell Identity. Immunity. 2020 Jul 14;53(1):217-232.e5.
27. Jahnmatz P, Sundling C, Yman V, Widman L, Asghar M, Sondén K, et al. Memory B-Cell Responses Against Merozoite Antigens After Acute Plasmodium falciparum Malaria, Assessed Over One Year Using a Novel Multiplexed FluoroSpot Assay. Front Immunol [Internet]. 2021 Feb 12 [cited 2024 Apr 22];11. Available from: https://www.frontiersin.org/journals/immunology/articles/10.3389/fimmu.2020.619398/full
28. Jahnmatz P, Nyabundi D, Sundling C, Widman L, Mwacharo J, Musyoki J, et al. Plasmodium falciparum-Specific Memory B-Cell and Antibody Responses Are Associated With Immunity in Children Living in an Endemic Area of Kenya. Front Immunol [Internet]. 2022 Mar 9 [cited 2024 Apr 22];13. Available from: https://www.frontiersin.org/journals/immunology/articles/10.3389/fimmu.2022.799306/full
29. Daniel PT, Krammer PH. Activation induces sensitivity toward APO-1 (CD95)-mediated apoptosis in human B cells. J Immunol. 1994 Jun 15;152(12):5624–32.
30. Peter ME, Budd RC, Desbarats J, Hedrick SM, Hueber AO, Newell MK, et al. The CD95 Receptor: Apoptosis Revisited. Cell. 2007 May 4;129(3):447–50.
31. Golinski ML, Demeules M, Derambure C, Riou G, Maho-Vaillant M, Boyer O, et al. CD11c+ B Cells Are Mainly Memory Cells, Precursors of Antibody Secreting Cells in Healthy Donors. Front Immunol [Internet]. 2020 Feb 25 [cited 2024 Apr 21];11. Available from: https://www.frontiersin.org/journals/immunology/articles/10.3389/fimmu.2020.00032/full
32. Johnson JL, Rosenthal RL, Knox JJ, Myles A, Naradikian MS, Madej J, et al. The Transcription Factor T-bet Resolves Memory B Cell Subsets with Distinct Tissue Distributions and Antibody Specificities in Mice and Humans. Immunity. 2020 May 19;52(5):842-855.e6.
33. Song W, Antao OQ, Condiff E, Sanchez GM, Chernova I, Zembrzuski K, et al. Development of Tbet- and CD11c-expressing B cells in a viral infection requires T follicular helper cells outside of germinal centers. Immunity. 2022 Feb 8;55(2):290-307.e5.
34. Urban BC, Hien TT, Day NP, Phu NH, Roberts R, Pongponratn E, et al. Fatal Plasmodium falciparum Malaria Causes Specific Patterns of Splenic Architectural Disorganization. Infect Immun. 2005 Apr;73(4):1986–94.
35. Harris PK, Yeoh S, Dluzewski AR, O'Donnell RA, Withers-Martinez C, Hackett F, et al. Molecular Identification of a Malaria Merozoite Surface Sheddase. PLOS Pathog. 2005 Nov 25;1(3):e29.
36. Fontana MF, Ollmann Saphire E, Pepper M. Plasmodium infection disrupts the T follicular helper cell response to heterologous immunization. Kurosaki T, Taniguchi T, Boyle MJ, editors. eLife. 2023 Jan 30;12:e83330.

37. Hong S, Zhang Z, Liu H, Tian M, Zhu X, Zhang Z, et al. B Cells Are the Dominant Antigen-Presenting Cells that Activate Naive CD4+ T Cells upon Immunization with a Virus-Derived Nanoparticle Antigen. Immunity. 2018 Oct 16;49(4):695-708.e4.
38. Arroyo EN, Pepper M. B cells are sufficient to prime the dominant CD4+ Tfh response to Plasmodium infection. J Exp Med. 2019 Nov 20;217(2):e20190849.
39. Gao X, Shen Q, Roco JA, Dalton B, Frith K, Munier CML, et al. Zeb2 drives the formation of CD11c + atypical B cells to sustain germinal centers that control persistent infection. Sci Immunol. 2024 Feb 8;eadj4748.
40. Ambegaonkar AA, Holla P, Dizon BL, Sohn H, Pierce SK. Atypical B cells in chronic infectious diseases and systemic autoimmunity: puzzles with many missing pieces. Curr Opin Immunol. 2022 Aug 1;77:102227.
41. Braddom AE, Bol S, Gonzales SJ, Reyes RA, Musinguzi K, Nankya F, et al. B Cell Receptor Repertoire Analysis in Malaria-Naive and Malaria-Experienced Individuals Reveals Unique Characteristics of Atypical Memory B Cells. mSphere. 2021 Sep 15;6(5):10.1128/msphere.00726-21.
42. Rask TS, Hansen DA, Theander TG, Pedersen AG, Lavstsen T. Plasmodium falciparum Erythrocyte Membrane Protein 1 Diversity in Seven Genomes – Divide and Conquer. PLOS Comput Biol. 2010 Sep 16;6(9):e1000933.
43. Amanna IJ, Carlson NE, Slifka MK. Duration of Humoral Immunity to Common Viral and Vaccine Antigens. N Engl J Med. 2007 Nov 8;357(19):1903–15.
44. Kilama M, Smith DL, Hutchinson R, Kigozi R, Yeka A, Lavoy G, et al. Estimating the annual entomological inoculation rate for Plasmodium falciparum transmitted by Anopheles gambiae s.l. using three sampling methods in three sites in Uganda. Malar J. 2014 Mar 21;13(1):111.
45. Kamya MR, Arinaitwe E, Wanzira H, Katureebe A, Barusya C, Kigozi SP, et al. Malaria Transmission, Infection, and Disease at Three Sites with Varied Transmission Intensity in Uganda: Implications for Malaria Control. Am J Trop Med Hyg. 2015 May 6;92(5):903–12.
46. Lau CKY, Turner L, Jespersen JS, Lowe ED, Petersen B, Wang CW, et al. Structural Conservation Despite Huge Sequence Diversity Allows EPCR Binding by the PfEMP1 Family Implicated in Severe Childhood Malaria. Cell Host Microbe. 2015 Jan 14;17(1):118–29.
47. Van Gassen S, Callebaut B, Van Helden MJ, Lambrecht BN, Demeester P, Dhaene T, et al. FlowSOM: Using self-organizing maps for visualization and interpretation of cytometry data. Cytometry A. 2015;87(7):636–45.